Bioconjugate Chemistry

Article

pubs.acs.org/bc

Incorporation of a Triglutamyl Spacer Improves the Biodistribution of Synthetic Affibody Molecules Radiofluorinated at the N-Terminus via Oxime Formation with ^{18}F-4-Fluorobenzaldehyde

Daniel Rosik,[†] Alf Thibblin,[‡] Gunnar Antoni,[‡,§] Hadis Honarvar,[∥] Joanna Strand,[∥] Ram Kumar Selvaraju,[§] Mohamed Altai,[∥] Anna Orlova,[§] Amelie Eriksson Karlström,[†] and Vladimir Tolmachev*[,∥]

[†]Division of Protein Technology, School of Biotechnology, KTH Royal Institute of Technology, Stockholm, Sweden

[‡]PET Centre, Uppsala University Hospital, Uppsala, Sweden

[§]Preclinical PET Platform, Uppsala University, Uppsala, Sweden

[∥]Unit of Biomedical Radiation Sciences, Rudbeck Laboratory, Uppsala University, Uppsala, Sweden

ABSTRACT: Affibody molecules are a class of affinity agents for molecular imaging based on a non-immunoglobulin protein scaffold. Previous studies have demonstrated high contrast for in vivo imaging of cancer-associated molecular abnormalities using Affibody molecules. Using the radionuclide ^{18}F for labeling and PET as the imaging modality, the sensitivity of molecular imaging using Affibody molecules can be further increased. The use of oxime formation between an aminooxy-functionalized peptide and ^{18}F-fluorobenzaldehyde (^{18}F-FBA) is a promising way of radiolabeling of targeting peptides. However, previous studies demonstrated that application of this method to Affibody molecules is associated with high liver uptake. We hypothesized that incorporation of a triglutamyl spacer between the aminooxy moiety and the N-terminus of a synthetic Affibody molecule would decrease the hepatic uptake of the ^{18}F-*N*-(4-fluorobenzylidine)oxime) (^{18}F-FBO)-labeled tracer. To verify this, we have produced two variants of the HER2-targeting $Z_{HER2:342}$ Affibody molecule by peptide synthesis: OA-PEP4313, where aminooxyacetic acid was conjugated directly to the N-terminal alanine, and OA-E_3-PEP4313, where a triglutamyl spacer was introduced between the aminooxy moiety and the N-terminus. We have found that the use of the spacer is associated with a minor decrease of affinity, from K_D = 49 pM to K_D = 180 pM. Radiolabeled ^{18}F-FBO-E_3-PEP4313 demonstrated specific binding to HER2-expressing ovarian carcinoma SKOV-3 cells and slow internalization. Biodistribution studies in mice demonstrated that the use of a triglutamyl linker decreased uptake of radioactivity in liver 2.7-fold at 2 h after injection. Interestingly, radioactivity uptake in kidneys was also reduced (2.4-fold). Experiments in BALB/C nu/nu mice bearing SKOV-3 xenografts demonstrated HER2-specific uptake of ^{18}F-FBO-E_3-PEP4313 in tumors. At 2 h pi, the tumor uptake (20 ± 2% ID/g) exceeded uptake in liver 5-fold and uptake in kidneys 3.6-fold. The tumor-to-blood ratio was 21 ± 3. The microPET/CT imaging experiment confirmed the biodistribution data. In conclusion, the use of a triglutamyl spacer is a convenient way to improve the biodistribution profile of Affibody molecules labeled at the N-terminus using ^{18}F-FBA. It provides a tracer capable of producing high-contrast images of HER2-expressing tumors.

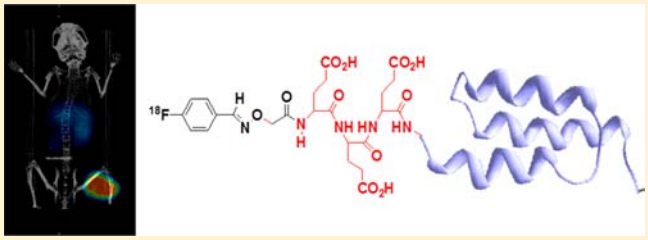

INTRODUCTION

Cancer proliferation, metastasis, and neoangiogenesis are often associated with overexpression and excessive signaling of certain transmembrane receptor tyrosine kinases (RTK).[1] Specific blocking or downregulation of these RTKs is a promising approach to therapy of disseminated cancer. Several RTK-targeting monoclonal antibodies and tyrosine kinase inhibitors have demonstrated improvement of cancer patients' survival and have been approved for routine clinical use. The major issue is, however, the heterogeneity of RTK over-expression. Only a fraction of the patients would have tumors expressing a particular RTK and potentially benefit from a certain treatment. Moreover, expression of RTKs can change during the course of the disease or in response to therapy. As overexpression of a molecular target often is a strong predictive and/or pharmacodynamic biomarker for response to targeting therapy, a noninvasive, repeatable determination of RTK expression levels in tumors would enable personalized therapy of cancer. Radionuclide molecular imaging of RTKs may be a facile method for patient stratification for targeting therapy.[2,3]

A precondition for the implementation of radionuclide imaging into clinical practice is having high sensitivity and specificity. The use of radiolabeled therapeutic antibodies is a straightforward way for imaging the expression of their molecular targets.[4] However, the long residence time of antibodies in circulation and slow extravasation and tissue penetration cause low tumor-to-organ radioactivity concentration ratios and, consequently, low contrast and sensitivity of

Received: July 23, 2013
Revised: December 15, 2013
Published: December 17, 2013

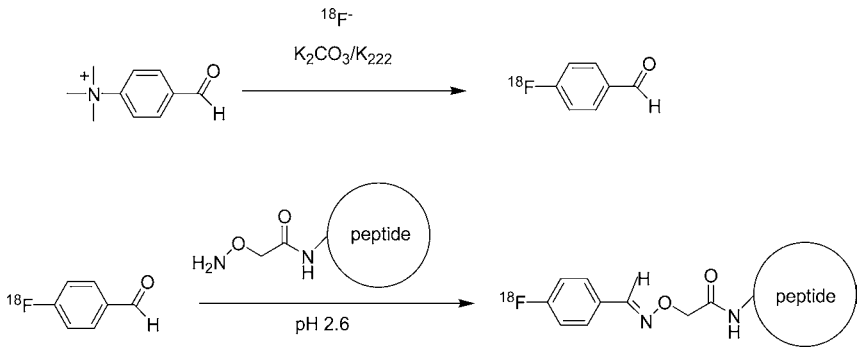

Figure 1. Radiofluorination of peptides using ^{18}F-FBA. For labeling of Affibody molecules, the aminooxy-linker was conjugated directly to the N-terminal alanine (PEP4313) or via a triglutamyl spacer (E_3-PEP4313).

imaging using radiolabeled antibodies.[3] Size reduction of targeting proteins is considered as a successful approach for increasing sensitivity of radionuclide imaging.[5] Both experimental data and theoretical calculation predict that molecular weights below 25 kDa in combination with high (at least low nanomolar) affinity are preconditions for successful targeting.[6] This prompts seeking an alternative to immunoglobulins as targeting agents.

A promising class of non-immunoglobulin-based targeting proteins are Affibody molecules, small (7 kDa), three-helix proteins based on the B-domain of protein A.[7] Currently, Affibody molecules with low nanomolar or subnanomolar affinity to several RTKs, e.g., HER2,[8] EGFR,[9] HER3,[10] PDGFRβ,[11] and IGF1R,[12] have been developed. Radiolabeled derivatives of the anti-HER2 $Z_{HER2:342}$ Affibody molecule have demonstrated the capacity of high contrast imaging of HER2-expressing tumors a few hours after injection both in preclinical studies[13] and in clinical trials.[14,15]Preclinical data suggest that derivatives of $Z_{HER2:342}$ provide the highest contrast (sensitivity) and specificity among all evaluated HER2 imaging agents.[13] Importantly, preclinical data demonstrated that different labeling approaches appreciably influence the biodistribution and targeting properties of Affibody molecules, and a careful optimization of the combination of nuclide and chelator or linker is required to obtain maximum imaging contrast.[16]

The use of positron-emitting labels should enable PET imaging and further increase the sensitivity of Affibody-mediated imaging. This is important for detection of expression in small metastases. The use of PET allows also an accurate quantification of uptake in tumor. For this reason, labeling of Affibody molecules with positron-emitting nuclides ^{11}C,[17] ^{18}F,[18−20] ^{64}Cu,[21] ^{68}Ga,[22,23] ^{76}Br,[24] and ^{124}I,[25] using different labeling strategies, has been evaluated.

^{18}F is one of the most attractive nuclides for labeling of Affibody molecules. Its half-life (109.5 min) is compatible with the rapid biokinetics of Affibody molecules. The short positron range of ^{18}F provides one of the best spatial resolutions among positron emitters. Due to the constant demand for ^{18}F-FDG, technologies for large scale production of ^{18}F and logistics for regional distribution of radiofluorinated tracers have been established. On the other hand, the chemistry for radiofluorination of proteins and peptides is demanding. The relative inertness of fluoride requires rather harsh labeling conditions, which necessitates the use of protected precursors. As a result, synthesis of reactive intermediates for fluorination of proteins was often a multi-step, time-consuming, and low-yield process.[26] However, several new promising approaches for radiofluorination of targeting proteins and peptides have been proposed during past decade. These approaches include formation of aluminum fluoride with subsequent chelation by triaza chelators (AlF chemistry),[27] the use of different variants of triazole formation by interaction of alkynes and azides ("click chemistry"),[28,29] ligation of radiofluorinated cyclooctene with a tetrazine by Diels−Alder reaction,[30] and oxime formation between an unprotected aminooxy-functionalized peptide and ^{18}F-labeled fluorobenzaldehyde (^{18}F-FBA)[31] (Figure 1). An important feature of such methods is a minimal number of synthetic steps with radiolabeled precursors. AlF chemistry provides residualizing labels and is the most suitable for peptides that are rapidly internalized after binding to cancer cells, although the same residualizing properties cause a prolonged retention of radioactivity in kidneys.[20] However, as internalization of the majority of anti-RTK Affibody molecules by cancer cells is slow,[9,12,22] nonresidualizing labels can be applied for their labeling without decreasing tumor uptake.

^{18}F-Fluorobenzaldehyde conjugation has been used for labeling of recombinant dimeric[19] and monomeric[32] anti-HER2 Affibody molecules (after conjugation of 2-(aminooxy)-*N*-(2-(2,5-dioxo-2,5-dihydro-1*H*-pyrrol-1-yl)ethyl)acetamide to a C-terminal cysteine) and a synthetic, truncated 2-helix variant of the anti-HER2 Affibody molecules.[33] All conjugates were capable of specific targeting of HER2-expressing xenografts in mice. However, a major concern in all cases was an elevated uptake of radioactivity in liver (close to or even exceeding uptake in tumors at 1−3 h pi), which would prevent imaging of liver metastases in clinics. Taking into account that liver is a major metastatic site for many tumors,[34] this is a serious issue. It has to be noted that the elevated liver uptake of ^{18}F-*N*-(4-fluorobenzylidine)oxime (^{18}F-FBO)-labeled Affibody molecules is associated with the labeling methods and not features of the Affibody molecules, as the same targeting proteins had several-fold lower hepatic uptake when labeled by other methods.[18,22,35] Furthermore, an elevated hepatic uptake or hepatobiliary excretion is often associated with either overall or local elevated lipophilicity of the protein surface.[36]Earlier, we have succeeded in the suppression of hepatic uptake or hepatobiliary excretion of Affibody molecules labeled with ^{99m}Tc at the N-terminus by increasing the hydrophilicity of the peptide-based chelators via incorporation of glutamyl residues.[37,38]

Our hypothesis was that incorporation of a triglutamyl spacer between the aminooxy moiety and the N-terminus of a synthetic Affibody molecule would decrease the hepatic uptake of ^{18}F-FBO-labeled Affibody molecules. To verify this, we have

dx.doi.org/10.1021/bc400343r | *Bioconjugate Chem.* 2014, 25, 82−92

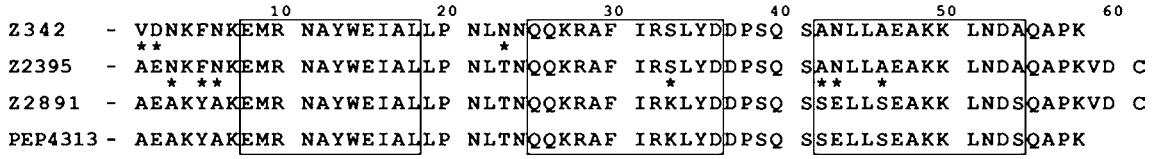

Figure 2. Alignment of the HER2-binding Affibody molecule (PEP4313) used in the present study and other variants of $Z_{HER2:342}$ described in the literature.[8,20,23] Asterisks indicate differences between aligned primary structures. Approximate positions of α-helices 1−3 are indicated by boxes.

produced two variants of the $Z_{HER2:342}$ Affibody molecule by peptide synthesis: OA-PEP4313, where aminooxy acetic acid was conjugated directly to N-terminal alanine, and OA-E_3-PEP4313, where a triglutamyl spacer was introduced between the aminooxy moiety and the N-terminus. Both variants and their *N*-(4-fluorobenzylidine)oxime derivatives were characterized by biophysical methods. Biodistribution of radiofluorinated variants was evaluated in normal mice to investigate the influence of the triglutamyl linker on hepatic uptake. In addition, targeting of HER2-expressing SKOV-3 xenografts using ^{18}F-FBO-E_3-PEP4313 was studied in immunodeficient mice by direct ex vivo measurements and microPET/CT imaging.

MATERIAL AND METHODS

Peptide Synthesis. The two Affibody molecules were based on the same core protein, PEP4313, where the only difference is a linker composed of three glutamate residues (E_3) introduced at the N-terminus (Figure 2).

The two molecules were synthesized using microwave-assisted solid-phase peptidesynthesis (SPPS). The assembly was performed on a fully automated peptide synthesizer with an integrated microwave oven (Liberty, CEM Corporation) as described earlier.[39] However, the Rink Amide MBHA LL resin (01-64-0467, Merck KGaA) was used in the current study. For deprotection, a 5% piperazine solution in *N*-methyl-2-pyrrolidone (NMP) was used with microwave irradiation. A 0.1 mmol batch was synthesized up to the first alanine (A1). Thereafter, the batch was split into two equal parts to prepare two different variants. At this stage, the triglutamyl (E3)-linker and the final, bis-Boc-protectedaminooxyacetic acid (BB-AOA) residue were attached using manual peptide synthesis. Briefly, the couplings were performed using 5 times molar excess of carboxylic acid. 9-Fluorenylmethyloxycarbonyl (Fmoc)-protected amino acid (Fmoc-AA) or BB-AOA, *O*-(benzotriazole-*N*,*N*,*N*′,*N*′-tetramethyluroniumhexafluorophosphate) (HBTU), and *N*-hydroxybenzotriazole (HOBt) in dimethylformamide (DMF) and *N*,*N*′-diisopropylethylamine (DIPEA) in NMP were added to the resin at a molar ratio of 1:1:1:2 (Fmoc-AA/HBTU/HOBt/DIPEA). The couplings were performed without microwave irradiation and using 20% piperidine solution for deprotection. The reactions were monitored using ninhydrin test to verify the absence of free amines, implying an incomplete reaction. During cleavage of the peptides using 95:2.5:2.5 trifluoroacetic acid (TFA)/H_2O/triisopropylsilane (TIS) for approximately 2 h at room temperature, 100 times molar excess of unprotected aminooxyacetic acid was added as a scavenger. The peptides were recovered using ether precipitation and finally freeze-dried before further purification.

Purification and Analysis. The crude peptides were purified on an Agilent 1100 HPLC system, using reversed phase HPLC (RP-HPLC). The purification was performed on a Zorbax 300SB C18 (9.4 mm × 250 mm, 5 μm) column using 0.1% TFA/$H_2O$and 0.1% TFA/CH_3CN as solvents A and B, respectively. The column oven temperature was set to 30 °C. The column was eluted with a linear gradient of 25% to 30% solvent B in 3 column volumes (CV) with flow rate of 5 mL/min. UV detection was at 220 and 280 nm, and 300 μL fractions were collected using an automated fraction collector. The fractions were analyzed on an Agilent 6500 Series Accurate-Mass Q-TOF LC/MS System using Agilent Mass Hunter Qualitative Analysis software version B.04.00. LC was run using a C4 column with the same buffers as the Agilent 1100 HPLC system. The fractions with correct mass were pooled, aliquoted, and freeze-dried. For final purity analysis, one aliquot of each protein was analyzed on the same Agilent 1100 HPLC system as earlier, using a Zorbax 300SB C18 (4.6 mm × 150 mm, 3 μm) column eluted with a linear gradient of 5% to 50% solvent B in 6 CV with flow rate of 1 mL/min.

It is important to mention that after the free aminooxyacetic acid (scavenger) has been removed, i.e., during and after purification of the peptides, all handling of the peptides was performed in glass or metal vessels, to avoid contact with plastic, which leads to extensive side reactions. Furthermore, organic solvents of high purity, free of contaminating carbonyl compounds, were used.

Conjugation of Nonlabeled FBA. For analytical purposes and for the development of a labeling protocol, purified aminooxy-peptides were conjugated with cold FBA. FBA (Sigma-Aldrich, no. 128376) was diluted 1000 times in methanol. The freeze-dried Affibody molecules were reconstituted in 0.1% TFA/H_2O, mixed with the diluted FBA in a molar ratio of 1:100 (Affibody/FBA), and incubated for 30 min at 60 °C. The reverse ratio (i.e., 100:1, Affibody/FBA) was also evaluated to mimic the conditions of the labeling reaction with ^{18}F-FBA. Analysis was performed using the same LC and LC/MS systems as described earlier.

Circular Dichroism (CD). FBO-E_3-PEP4313 and FBO-PEP4313 were analyzed by variable temperature measurements from 20 to 90 °C at 221 nm as described earlier.[40] A circular dichroism (CD) wavelength scan from 250 to 195 nm was collected before and after melting.

Biacore Analysis. The equilibrium dissociation constants (K_D) were determined by binding kinetics analysis on a Biacore 2000 instrument as described earlier.[40] The two protein variants were studied after conjugation to cold FBA. The extracellular domain of HER2 (rhErbB2/Fc, Pierce 1129ER) was immobilized on a CM5 sensor chip by amine coupling. Immobilization levels reached 1,000 response units (RU). The different Affibody molecules were diluted to concentrations ranging from 0.2 to 16 nM in HBS-EP buffer (0.01 M HEPES, pH 7.4, 0.15 M NaCl, 3 mM EDTA, 0.005% surfactant P20) from Biacore. The binding kinetics were studied in a 5-min association phase and a 30-min dissociation phase with a flow rate of 50 μL/min, followed by regeneration with 25 mMHCl. A 1:1 Langmuir binding model was used for the kinetic calculations. BIAEvaluation 4.1 software was used for calculations.

Radioactivity Measurements. Radioactivity was measured using a VDC-405 dose calibrator (Veenstra Instruments BV, The Netherlands) equipped with an ionization chamber. In animal studies, the radioactivity was measured using an automated gamma-counter with a 3-in. NaI(Tl) detector. The distribution of radioactivity along the ITLC strips was measured on the Cyclone Storage Phosphor System (Packard) and analyzed using the OptiQuant image analysis software (OptiQuant).

Radiolabeling. The semipreparative HPLC purification was performed with a VWR HPLC system with a VWR LaPrep P110 gradient pump and a LaPrep P311 variable wavelength UV detector in series with a Bioscanβ+ flow radioactivity detector FC-3600. The semipreparative HPLC purification was carried out on an ACE C18 HL (250 mm × 10 mm, 5 μm) column with 40% MeCN in water, flow 5 mL/min. The analytical HPLC analyses were performed using a VWR-Hitachi LaChrom Elite system with an L-2130 gradient pump, an L-2300 autosampler, and an L-2450 diode-array detector in series with a BioscanFC-3300 γ flow count radioactivity detector. The product analysis was performed using Zorbax 300SB C18 column calibrated using nonlabeled FBO-E3-PEP4313 and FBO-PEP4313.

^{18}Fluoride anion was produced via the ^{18}O(p,n)^{18}F nuclear reaction using a Scanditronix MC17 cyclotron. The bombardment of enriched ^{18}O water (98%, Rotem) gave an aqueous solution of $^{18}F^-$, which was transferred from the cyclotron target with a flow of CH_3CN/H_2O (35:65 v/v) and trapped on a preconditioned QMA column (Waters). The column was purged with helium and then eluted with a solution of Kryptofix K222 (900 μL, 10 mg/mL) and potassium carbonate (1.4 mg/mL) in CH_3CN/H_2O 80:20 v/v. The eluate was dried at 120 °C under a stream of helium. After drying, a procedure that took about 23 min, the ^{18}F-Kryptofix complex was used directly for the nucleophilic aromatic substitution of the precursor.

Radiofluorination was performed as described by Poethko and co-workers.[31] The radiosyntheses were carried out at the PET Centre at Uppsala University Hospital, on an in-house built Synthia robot system based upon a Gilson ASPEC module. The 4-formyl-*N*,*N*,*N*-trimethylanilinium triflate (3.0 mg) dissolved in 1000 μL of dry DMSO was added to the dried ^{18}F-Kryptofix complex. The reaction mixture was heated at 100 °C for 15 min and then cooled 1.5 min with compressed air before the next step. The radiochemical yield as measured by HPLC was 50−70%. The labeled aldehyde was purified with reversed-phase semipreparative HPLC.

An HPLC fraction (2.9 mL, 40% CH_3CN in H_2O) containing purified labeled aldehyde was added to the peptide precursor (108 μg) dissolved in 900 μL of a citrate/phosphate/CH_3CN solution, pH 2.6. After 15 min at 70 °C, the mixture was cooled for 1.5 min with compressed air and then transferred to a rotary evaporator. About 80% of the solvent was removed at reduced pressure and heating (95 °C). This procedure removes the labeled aldehyde almost quantitatively (see below). Water (5 mL) was added before further purification.

A final purification and solvent exchange was performed using NAP-5 size-exclusion column, pre-equilibrated and eluted with PBS. The radiochemical purity of the final product was determined by ITLC eluted with acetone/water (80:70). In this system, radiolabeled Affibody molecules remain at application point while fluorobenzaldehyde and fluoride migrates with the solvent front.

In Vitro Binding Specificity and Cellular Processing. Binding specificity and cellular processing of ^{18}F-FBO-E_3-PEP4313 was studied using HER2-expressing ovarian carcinoma SKOV-3 cells (1.6×10^6 receptors/cells[41]). ^{18}F-FBO-E_3-PEP4313 at a protein concentrations of 270 pM was added to 6 dishes (10^6 cells/dish). A 1000-fold excess of nonlabeled recombinant parental Affibody molecule was added to 3 of the Petri dishes 5 min before the labeled conjugate to saturate the receptors. The dishes were incubated for 1 h in a humidified incubator at 37 °C. The media was collected, the cells were detached using trypsin-EDTA solution, and the radioactivity was measured both in the media and the cell suspension. The percentage of cell-bound radioactivity was calculated for both the presaturated and unsaturated cells.

Processing of the^{18}F-FBO-E_3-PEP4313 by SKOV-3 cells during continuous incubation was studied according to a method described and validated by Wållberg and co-workers.[42] The labeled compounds (protein concentration of 1 nM) were added to Petri dishes containing 10^6 cells/dish. The cells were incubated at 37 °C, in a humidified atmosphere containing 5% CO_2. At predetermined time points (1, 2, 3, and 4 h after incubation start), the media from 3 dishes was collected and the cells were washed in ice-cold serum-free medium. The cells were then treated with 0.5 mL of 0.2 M glycine buffer containing 4 M urea, pH 2.5, for 5 min on ice. The solution was collected, and the cells were washed additionally with 0.5 mL of glycine buffer. The fractions were pooled together. The radioactivity of the acid wash fractions was considered to be membrane-bound radioactivity. The cells were then incubated at 37 °C for at least 30 min with 0.5 mL of 1 M NaOH. The alkaline solution was collected, the cell dishes were washed with an additional 0.5 mL of NaOH, and the alkaline fractions were pooled. The radioactivity in the alkaline fractions was considered as internalized. A percentage of the internalized radioactivity was calculated for each fraction at each time point.

Biodistribution Studies. The animal study was approved by the Local Ethics Committee for Animal Research. The animals were acclimatized for one week at the Rudbeck laboratory animal facility before experiments.

For comparative biodistribution study, normal female NMRI mice were used. An average animal weight was 30 ± 2 g at the time of experiment. The radiochemical purity of injected conjugate was 99.9% and 99.7% for ^{18}F-FBO-PEP4313 and^{18}F-FBO-E_3-PEP4313, respectively. Mice (group of four) were intravenously injected with ^{18}F-FBO-PEP4313 or ^{18}F-FBO-E_3-PEP4313 (~60 kBq in 100 μL of PBS). The total injected amount of protein was adjusted to 1 μg per animal by adding unlabeled protein. The mice were euthanized at 2 h pi with an intraperitoneal injection of Ketalar-Rompun solution (20 μL of solution per gram of body weight: Ketalar [ketamine], 10 mg/mL; Rompun [xylazin], 1 mg/mL). Thereafter, mice were exsanguinated by syringes rinsed with diluted heparin. Blood and organ samples (lung, liver, spleen, kidney, muscle, and bone) were collected and weighed. Their radioactivity was measured using an automatic gamma-counter. A standard of injected activity was also measured along with each group of mice. The organ uptake values were calculated as percent injected dose per gram tissue (% ID/g). The whole gastrointestinal tract was taken from each animal to determine a level of hepatobiliary excretion of radioactivity. An unpaired Student's *t* test was used to determine a significant difference ($p < 0.05$) between uptake of ^{18}F-FBO-PEP4313 and ^{18}F-FBO-E_3-PEP4313.

dx.doi.org/10.1021/bc400343r | *Bioconjugate Chem.* 2014, 25, 82−92

Targeting properties of different conjugates were compared in female BALB/c nu/nu mice (15 weeks old, mean weight of 20.0 ± 1.5 g) carrying SKOV-3 xenografts. The cells (10^7 cells per mouse) were subcutaneously implanted in the right hind leg 5 weeks before the experiment. At the time of the experiment, an average tumor weight was 0.19 ± 0.1 g. ^{18}F-FBO-E_3-PEP4313 in 100 μL of PBS each was injected in two groups of mice (four mice each). The radiochemical purity of the injected conjugate was 99.7%. The activity of ^{18}F-FBO-E_3-PEP4313 was 40 kBq/mouse for the group sacrificed at 1 h pi, and 60 kBq/mouse for the group sacrificed at 2 h pi. The total injected amount of protein was adjusted to 1 μg/animal by adding unlabeled protein. In order to check the specificity of in vivo targeting, HER2 receptors in one additional group of mice were saturated by the injection of 750 μg of unlabeled recombinant $Z_{HER2:342}$ Affibody molecule 40 min before the injection of ^{18}F-FBO-E_3-PEP4313 (60 kBq/mouse, 1 μg/mouse). These mice were sacrificed at 2 h after injection. The biodistribution was measured as described above.

Imaging. To confirm the capacity of ^{18}F-FBO-E_3-PEP4313 to image HER2-expressing tumors, two mice bearing SKOV-3 xenografts were intravenously injected with 2.5 MBq of ^{18}F-FBO-E_3-PEP4313 (3.3 μg peptide). Immediately before imaging (1 or 2 h pi), the animals were euthanized, and the urine bladders were dissected. The PET/CT imaging was performed in The Triumph Trimodality system (Gamma Medica, Inc.), a fully integrated SPECT/PET/CT hardware and software platform optimized for small animals. The PET data was reconstructed into a static image using a MLEM 2D algorithm (10 iterations). The CT raw file was reconstructed using Filter Back Projection (FBP). PET and CT dicom-files were analyzed using PMOD v 3.12 software (PMOD Technologies Ltd., Zurich, Switzerland).

RESULTS

Peptide Synthesis. Aminooxy derivatives of PEP4313 were successfully synthesized using Fmoc solid-phase peptide synthesis followed by manual conjugation of Bis-Boc-aminooxyacetic acid with subsequent deprotection. The mass of each peptide was determined by ESI-MS, and the experimentally determined molecular weights correlated well with the theoretically calculated values (Figure 3). Conjugation of nonlabeled FBA provided yields of almost 70% when an excess of FBA was used. After a simple size-exclusion chromatography using a disposable NAP-5 column, no free FBA could be detected. After confirming the molecular weight by mass spectrometry, FBO-PEP4313 and FBO-E_3-PEP4313 were used as standards for radio-HPLC.

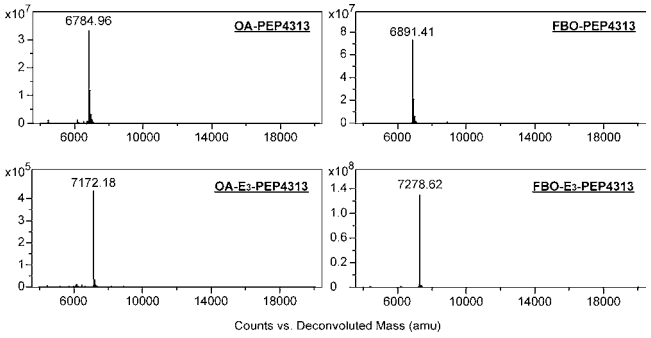

Figure 3. Deconvolution results from MS for OA-PEP4313, FBO-PEP4313, OA-E_3-PEP4313, and FBO-E_3-PEP4313. The measured masses were in good accordance with the theoretical values (6784.6, 7172.0, 6890.7, and 7278.1 for OA-PEP4313, OA-E_3-PEP4313, FBO-PEP4313, and FBO-E_3-PEP4313, respectively).

Circular dichroism (CD) spectra of FBO-PEP4313 and FBO-E_3-PEP4313 before and after heating are presented in Figure 4. Both conjugates generated very similar spectra typical for α-helical structures. The CD spectra did not show any noticeable difference in secondary structure content before and after heating to 90 °C for either of the constructs, indicating accurate refolding after denaturing. The melting point (TM) was determined to be 72 and 73 °C for FBO-PEP4313 and FBO-E_3-PEP4313, respectively.

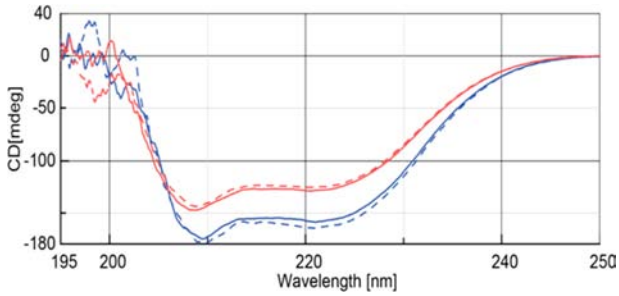

Figure 4. CD spectra showing FBO-E_3-PEP4313 in red and FBO-PEP4313 in blue. The dashed lines are before heating to 90 °C, and solid lines are after heating.

Biacore Analysis. Using Biacore analysis the binding affinity of FBO-E_3-PEP4313 to HER2 protein was estimated to be K_D = 180 pM ($k_a = 2.2 \times 10^6$ M s^{-1}, $k_d = 3.8 \times 10^{-4}$ s^{-1}), while the corresponding K_D for FBO-PEP4313 was 49 pM ($k_a = 6.6 \times 10^6$ M s^{1-}, $k_d = 3.3 \times 10^{-4}$ s^{-1}).

Radiolabeling. An unoptimized labeling procedure provided an overall non-decay-corrected yield of 3−5%. The simple azeotropic evaporation of unreacted ^{18}F-fluorobenzaldehyde resulted in a radiochemical purity of radiofluorinated Affibody molecules of 97% (Figure 5). An additional purification and buffer exchange using disposable NAP-5 size-exclusion columns provided a purity of over 99%.

The binding specificity test demonstrated that adding an excess of unlabeled recombinant $Z_{HER2:342}$ Affibody molecule reduced binding of ^{18}F-FBO-E_3-PEP4313 to HER2-expressing SKOV-3 cells from 49 ± 5% of added radioactivity to 0.39 ± 0.07% ($p < 5 \times 10^{-5}$). This demonstrates the saturability of the binding and suggests receptor-mediated binding of ^{18}F-FBO-E_3-PEP4313 to HER2-expressing cells.

Data for the cellular processing of ^{18}F-FBO-E_3-PEP4313 by HER2-expressing SKOV-3 cells are presented in Figure 6. The processing patterns were typical of $Z_{HER2:342}$ and its derivatives. The binding was very rapid, and the uptake plateau was reached within 1 h. The internalization was slow. The internalized fraction of activity was small (5−6% of totally bound activity) and did not increase with time.

Animal Study. Data concerning a comparative biodistribution of ^{18}F-FBO-PEP4313 and ^{18}F-FBO-E_3-PEP4313 in NMRI mice at 2 h pi are presented in Figure 7. Both compounds demonstrated a rapid clearance from blood (less than 1% ID/g at 2 h pi) and the majority of organs and tissues. The radioactivity in the gastrointestinal tract and its content was lower than 4% of the injected radioactivity, which suggests that the hepatobiliary pathway played a minor role in excretion of

dx.doi.org/10.1021/bc400343r | Bioconjugate Chem. 2014, 25, 82−92

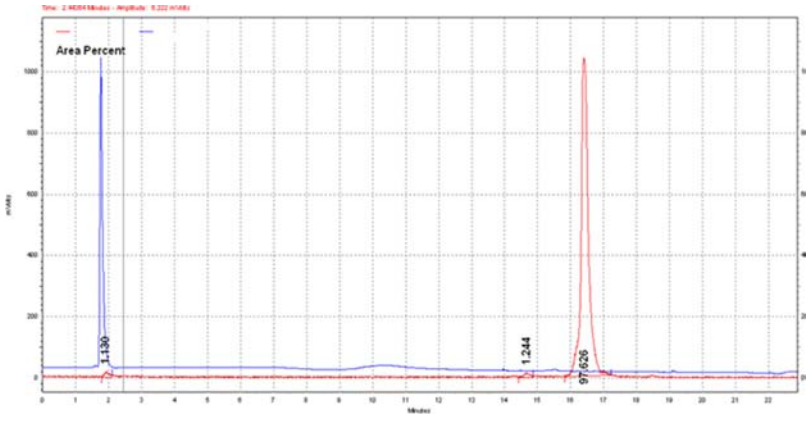

Figure 5. Representative radio-HPLC chromatogram (^{18}F-FBO-E_3-PEP4313) of radiolabeled Affibody molecule after evaporation of ^{18}F-fluorobenzaldehyde. The blue line shows the signal from the UV detector, and the red line is from the radioactivity detector. The retention time of the main radioactivity peak corresponds to the retention time of nonlabeled FBO-E_3-PEP4313.

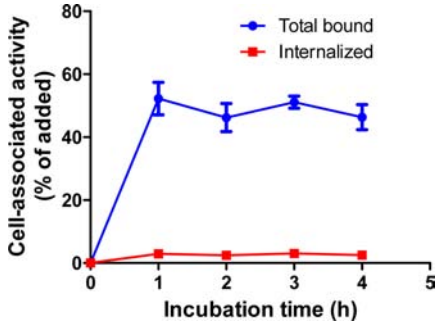

Figure 6. Cellular processing of ^{18}F-FBO-E_3-PEP4313 by HER2-expressing cells (SKOV-3) in vitro. Cells were incubated with labeled compound at 37 °C. Data are presented as mean values for three cell dishes with standard deviations. Error bars may be smaller than the symbols.

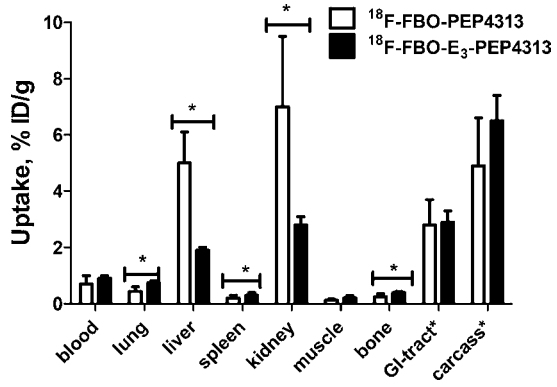

Figure 7. Comparative biodistribution of ^{18}F-FBO-PEP4313 and ^{18}F-FBO-E_3-PEP4313 in NMRI mice at 2 h pi Data expressed as % ID/g and presented as an average with standard deviation for four mice. Asterisk indicates a significant difference ($p < 0.05$ in a Student's t test) between uptake of ^{18}F-FBO-PEP4313 and that of ^{18}F-FBO-E_3-PEP4313. Data for gastrointestinal tract (with content) and carcass are provided as % ID per whole sample.

both radiofluorinated conjugates. The hepatic uptake of ^{18}F-FBO-E_3-PEP4313 (1.9 ± 0.1% ID/g) was 2.7-fold lower ($p < 0.5$) than the uptake of ^{18}F-FBO-PEP4313 (5.0 ± 1.1% ID/g). The renal retention of radioactivity was also lower (2.4-fold, $p < 0.5$) for ^{18}F-FBO-E_3-PEP4313. However, uptake of ^{18}F-FBO-E_3-PEP4313 in lung, spleen, and bones was approximately 1.5-fold higher.

Results of the biodistribution experiments of ^{18}F-FBO-E_3-PEP4313 in BALB/c nu/nu mice bearing SKOV-3 xenografts are presented in Figures 8, 9, and 10.

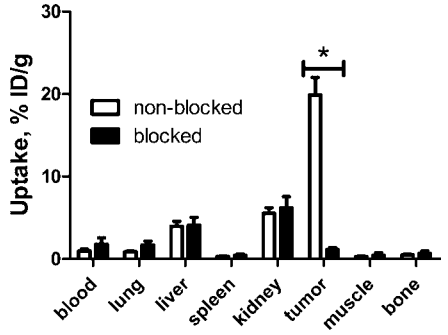

Figure 8. In vivo targeting specificity of SKOV-3 xenografts using ^{18}F-FBO-E_3-PEP4313 at 2 h pi. One group of animals was preinjected with 750 μg of nonlabeled $Z_{HER2:342}$ to saturate the HER2 receptors 40 min before injection of the radiolabeled conjugate. Results are expressed as % ID/g and as average values for four mice with standard deviation. Saturation of the HER2 receptors in the tumor caused a significant ($p < 5 \times 10^{-6}$) decrease of radioactivity uptake in tumors.

In order to verify the specificity of ^{18}F-FBO-E_3-PEP4313 accumulation in HER2-expressing SKOV-3 xenografts, its biodistribution at 2 h pi was studied after saturating the binding epitope of HER2 by preinjection of a large excess of nonlabeled $Z_{HER2:342}$ (Figure 8). The blocking of the binding sites reduced the tumor uptake from 20 ± 2% to 1.2 ± 0.2% ID/g ($p < 5 \times 10^{-6}$), demonstrating the specificity of HER2 targeting.

The biodistribution data for BALB/c nu/nu mice (Figure 9A) were in a good agreement with the data for NMRI mice (Figure 7), taking into account the much smaller size of the tumor-bearing mice. Already at 1 h after injection, radioactivity was cleared to a high extent from blood and the majority of tissues (Figure 9 A). At the same time, the tumor uptake was 21 ± 3% ID/g, and only the uptake in kidneys was higher. At 2 h after injection, the tumor uptake (20 ± 2% ID/g) did not differ significantly from uptake at 1 h after injection, but radioactivity was further cleared from blood (3.5-fold reduction) and all other measured organs and tissues. The most pronounced

dx.doi.org/10.1021/bc400343r | Bioconjugate Chem. 2014, 25, 82−92

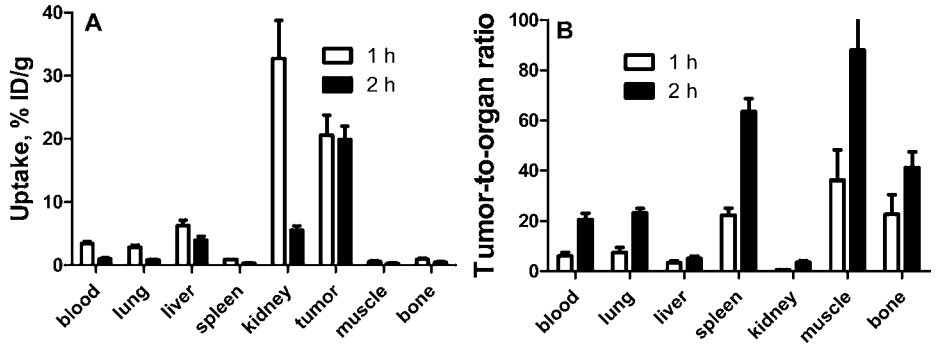

Figure 9. Biodistribution expressed as % ID/g (A) and tumor-to-organ ratios (B) of ^{18}F-FBO-E_3-PEP4313 in BALB/C nu/nu mice bearing SKOV-3 xenografts. Data are presented as average value for four mice with standard deviation.

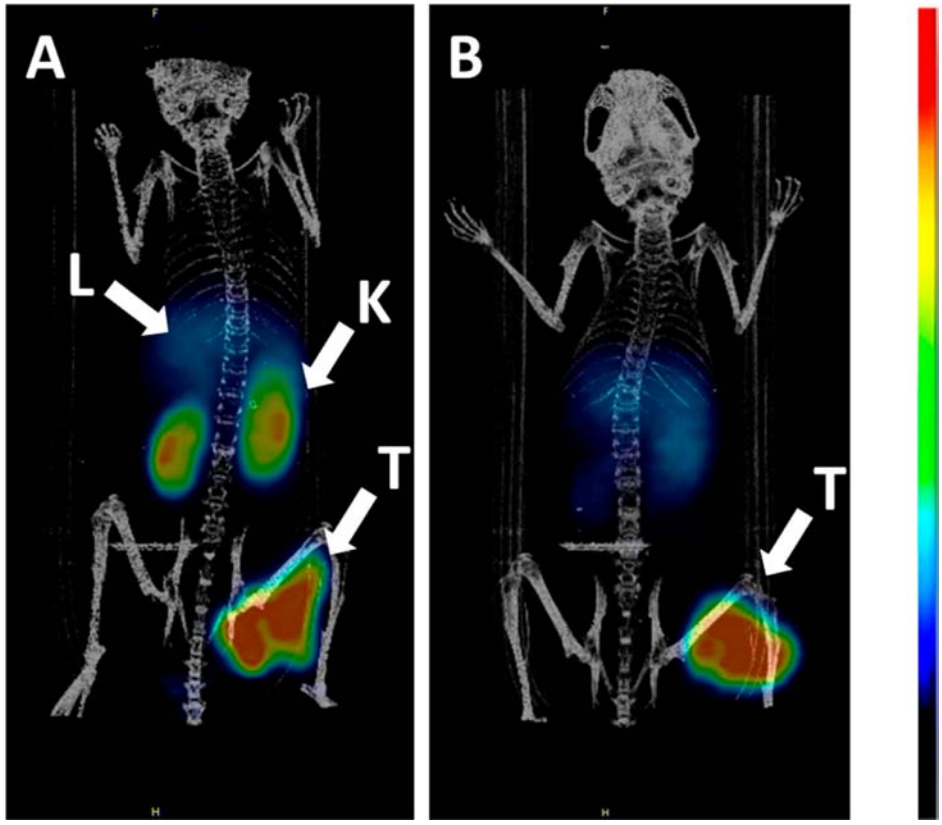

Figure 10. Coronal microPET/CT images (MIP) of mice bearing SKOV-3 xenografts at 1 h (A) and 2 h (B) after injection of ^{18}F-FBO-E3-PEP4313. Arrows point at tumor (T), liver (L), and kidney (K).

difference, nearly 6-fold, was the reduction of renal uptake. The hepatic uptake was reduced 1.6-fold. This resulted in appreciable increase of tumor-to-organ ratios. At 2 h after injection, the tumor-to-blood, tumor-to-liver, and tumor-to-kidney ratios were 20 ± 2, 5.1 ± 0.8, and 3.6 ± 0.6, respectively.

The microPET/CT experiment (Figure 10) confirmed the results of the biodistribution study. Already at 1 h after injection, radioactivity in the tumor and kidneys dominated the image (Figure 10A) and average liver uptake was ca. 3-fold lower than in the tumor. By 2 h after injection (Figure 10B), the radioactivity was cleared from the kidneys, and the tumor was the only site with pronounced radioactivity accumulation.

■ DISCUSSION

A steadily increasing amount of scientific data suggest that Affibody molecules is a promising class of targeting proteins that can be successfully applied for radionuclide imaging of molecular targets for cancer therapy, particularly RTKs (for reviews see refs 3 and 13). The combination of the exquisite specificity of the Affibody molecules and the high resolution, sensitivity, and quantification accuracy of PET would further improve in vivo imaging of cancer-related molecular abnormalities. The use of ^{18}F as a label would facilitate translation of Affibody-based imaging agents into clinical practice due to the availability of this nuclide and the good feasibility of regional distribution of radiofluorinated tracers. However, a careful optimization of labeling chemistry and molecular design of Affibody molecules is required to realize the potential of these targeting proteins for radionuclide imaging. Importantly, sensitivity of imaging is dependent on contrast, which is determined by tumor-to-organ ratios. That is why a reduction of radioactivity uptake in normal organs and

dx.doi.org/10.1021/bc400343r | Bioconjugate Chem. 2014, 25, 82−92

tissues is as important as enhancement of uptake in tumors. This study was dedicated to the reduction of radioactivity uptake in liver, an important metastatic site for many cancers.

We have shown earlier that incorporation of amino acids with hydrophilic, preferably negatively charged, side chains into mercaptoacetyl-containing peptide-based chelators for labeling with $^{99m}Tc{=}O^{+3}$ [37] and histidine-based chelators for labeling with $[^{99m}Tc(CO)_3]^{+}$ [38] reduces hepatic uptake and hepatobiliary excretion of Affibody molecules. This led us to the hypothesis that the use of a triglutamyl spacer between an Affibody molecule and aminooxy-containing moiety for labeling with ^{18}F-FBA might also have a similar effect. However, the molecular mechanism behind the reduction of hepatic uptake of Affibody molecules labeled with ^{99m}Tc using glutamate-containing chelators is unclear. Moreover, there is a profound chemical and structural difference between the ^{99m}Tc chelates and the ^{18}F-FBO label conjugated via triglutamyl spacer (Figure 11). Earlier studies suggested that much smaller differences,

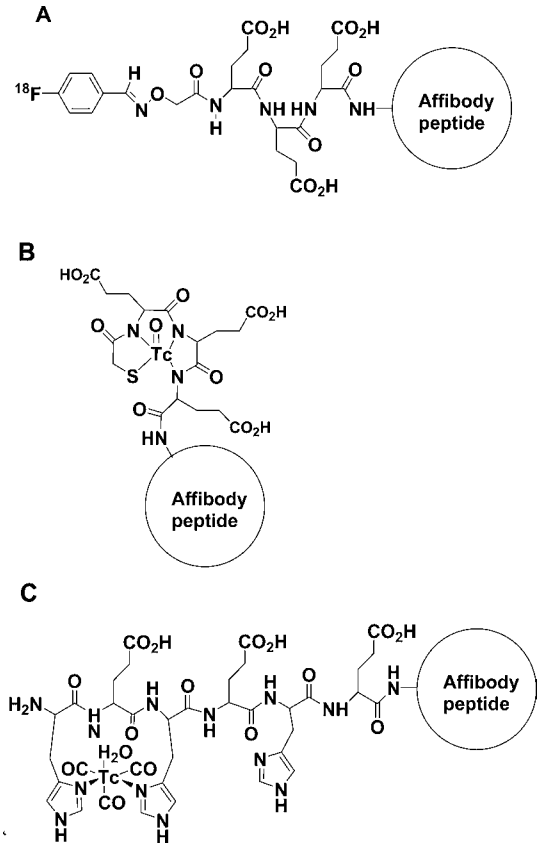

Figure 11. Schematic drawing of Affibody molecules labeled with (A) ^{18}F-*N*-(4-fluorobenzylidine)oxime) using a triglutamate spacer, (B) $^{99m}Tc{=}O^{3+}$ using mercaptoacetyl-Glu-Glu-Glu-chelator,[34] and (C) $[^{99m}Tc(CO)_3]^{+}$ using His-Glu-His-Glu-His-Glu-chelator.[35]

e.g., the use of the homologous macrocyclic chelators DOTA, NOTA, and NODAGA, had appreciable influence on the biodistribution (including hepatic uptake) of Affibody molecules labeled with ^{111}In and ^{68}Ga.[43] Thus, achieving of the desirable effect was not given a priori. The reduction of the hepatic uptake of ^{18}F-labeled Affibody molecules required not only changes in the labeling chemistry but also biological re-evaluation of modified imaging agents.

The triglutamyl spacer did not reduce the melting point of the protein. The presence of the spacer had no influence on the capacity of FBO-E_3-PEP4313 to refold after heating to 90 °C (Figure 4). This suggested that rather harsh labeling conditions are still permissible to this protein.

Conjugation of FBA was swift and efficient under the right conditions with low pH and elevated temperatures. However, great care has to be taken in order to prevent the reactive aminooxy group on the peptides not to produce side reactions in contact with plastics. In our hands, contact with different types of plastics (e.g., polypropylene, PEEK, and polyethylene) added a +12 Da adduct to the peptides within 1 h. Our hypothesis is that the aminooxy group reacted with residual formaldehyde on the plastic walls, which would add 12 Da to the total mass after formation of the corresponding oxime. Avoiding any contact with plastics from the first purification to the point of conjugation with FBA seemed to eliminate the side reaction and produce constructs with expected masses according to the theoretical calculations.

Importantly, both FBO-PEP4313 and FBO-E_3-PEP4313 retained the capacity to bind to HER2 with very high (low picomolar) affinity. Apparently, incorporation of the triglutamyl spacer reduced the on-rate of the binding, which caused increase of the dissociation constant from 49 pM for FBO-PEP4313 to 180 pM for FBO-E_3-PEP4313. This was not entirely unexpected, as N-terminal modification has earlier caused some modulation of affinity of Affibody molecules.[37,43] However, our recent study[41] has demonstrated that a reduction of affinity of an Affibody molecule from K_D = 120 pM to K_D = 3.8 nM has no influence on the uptake of radiolabeled anti-HER2 Affibody molecules in tumors with high HER2 expression at 4 h after injection. Even in the case of low target expression, there was no difference in uptake of Affibody molecules with affinities of K_D = 116 and K_D = 154 pM at early time points.[41]The biodistribution and imaging studies (Figures 8, 9, and 10) confirmed the excellent targeting properties of ^{18}F-FBO-E_3-PEP4313. It should be noted, however, that the influence of a spacer on a binding site should depend on the binding site composition and might differ for Affibody molecules specific to different molecular targets.

The biodistribution experiment confirmed the correctness of our hypothesis. The uptake of ^{18}F-FBO-E_3-PEP4313 in liver was nearly 3-fold ($p < 0.05$) lower than the uptake of ^{18}F-FBO-PEP4313 (Figure 7). Thus, the use of a triglutamyl extension of the N-terminus permits modulation of the hepatic uptake of Affibody molecules. Interestingly, there was no significant difference in the radioactivity in the gastrointestinal tract. This means that the presence of the spacer did not influence hepatobiliary excretion of radioactivity. Most likely, the radiocatabolites of both conjugates do not act as substrates for efflux pumps on apical (canalicular) membrane of hepatocytes.

Reduction of the renal uptake was an interesting effect of the spacer. Unlike Affibody molecules labeled using residualizing radiometal labels,[22,23,35,38] the renal retention of ^{18}F-*N*-(4-fluorobenzylidine)oxime-labeled Affibody molecules is quite low (Figure 9). This is in agreement with data showing rapid clearance of radioactivity from kidneys for other Affibody molecules labeled with ^{18}F-*N*-(4-fluorobenzylidine)-oxime.[19,32,33] This is a strong indication that the ^{18}F-*N*-(4-fluorobenzylidine)oxime-label is nonresidualizing, i.e., its hydrophobic radiocatabolites leak from the cell after intracellular proteolytic degradation of the Affibody molecules. One possible explanation for the difference in the renal retention of ^{18}F-FBO-E_3-PEP4313 and ^{18}F-FBO-PEP4313 is that the presence of a

dx.doi.org/10.1021/bc400343r | *Bioconjugate Chem.* 2014, 25, 82−92

triglutamyl spacer facilitates enzymatic cleavage of hydrophobic ^{18}F-bearing catabolites from the Affibody molecule during processing in the proximal tubuli cells and, in this way, makes the clearance process more rapid. Another possible explanation is based on the fact that the reabsorption of peptides in the kidneys is mediated by interaction of "negative patches" on the proximal tubuli cells with positively charged side chains of peptides.[44] The presence of the negatively charged spacer might interfere with such an interaction and reduce the renal reabsorption of ^{18}F-FBO-E_3-PEP4313 in comparison with that of ^{18}F-FBO-PEP4313. Whatever the explanation, such a feature would facilitate imaging of adrenal metastases and other metastases in the lumbar area.

Experiments in tumor-bearing mice confirmed that ^{18}F-FBO-E_3-PEP4313 can target HER2-expressing xenografts with high specificity (Figure 8). The tumor uptake appreciably exceeded the hepatic uptake already at 1 h after injection and renal uptake at 2 h because of radioactivity clearance from these organs (Figures 9 and 10). The tumor uptake remained unchanged between the two time points, despite the apparent nonresidualizing properties of the label. Apparently, this is due to slow internalization of ^{18}F-FBO-E_3-PEP4313 by tumor cells (Figure 6).

It has to be noted that the renal uptake of ^{18}F-FBO-E_3-PEP4313 at 2 h after injection (5.5 ± 0.7% ID/g) in the second animal study (Figures 8 and 9) was higher than in the first one (2.8 ± 0.3% ID/g, Figure 7). However, the models were not the same in these two studies. In the first study, the goal was to compare biodistributions of ^{18}F-FBO-PEP4313 and ^{18}F-FBO-E_3-PEP4313 in normal organs, and the use of cheap normal NMRI mice (average weight of 30 ± 2 g) was reasonable, as both variants were assessed in the same model. In the second study, immunodeficient BALB/C nu/nu mice (average weight of 20.0 ± 1.5 g) were used because we aimed to use tumor xenografts. The BALB/C nu/nu mice were 1.5-fold smaller than NMRI, and therefore the kidneys were smaller, which resulted in higher uptake per gram of tissue. Furthermore, the difference in the renal uptake of ^{18}F-FBO-E_3-PEP4313 in nude mice at 1 h (33 ± 6% ID/g) and 2 h (5.5 ± 0.7% ID/g) after injection suggests that renal catabolism plays a noticeable role in the release of radioactivity from kidneys. The catabolism in nude mice is much less active than in normal mice.[45] In our previous studies, we have observed that the renal retention of radioactivity of the same conjugates is higher in nude mice than in normal mice when renal catabolism and excretion of radiometabolies played a substantial role.[46−48] Thus a combination of these two factors (smaller kidney size and slower renal catabolism in nude mice) may explain the difference in renal uptake in normal and nude mice.

Table 1 shows a comparison of tumor-to-organ ratios of ^{18}F-FBO-E_3-PEP4313 with tumor-to-organ ratios of ^{68}Ga-DOTA-$Z_{HER2:342}$ anti-HER2 Affibody molecule[22] in BALB/C nu/nu mice bearing SKOV-3 xenografts at 2 h pi. ^{68}Ga-DOTA-$Z_{HER2:342}$ has demonstrated a capacity for a high-contrast imaging of HER2-expressing breast cancer metastases in clinics.[14] Apparently, the tumor-to-organ ratios of ^{18}F-FBO-E_3-PEP4313 were quite similar to those of a radiometal-labeled counterpart having the highly hydrophilic DOTA chelator at the N-terminus. The renal uptake of ^{18}F-FBO-E_3-PEP4313 is nearly 100-fold lower, which resulted in much higher tumor-to-kidney ratio for the radiofluorinated tracer. This comparison suggests that ^{18}F-FBO-E_3-PEP4313 has a favorable biodistribution profile for radionuclide imaging in vivo.

Table 1. Comparison of Tumor-to-Organ Ratios for ^{18}F-FBO-E_3-PEP4313 and ^{68}Ga-DOTA-$Z_{HER2:342}$ in BALB/C nu/nu Mice Bearing SKOV-3 Xenografts at 2 h pi[a]

	tumor-to-organ ratio	
	^{18}F-FBO-E_3-PEP4313	^{68}Ga-DOTA-$Z_{HER2:342}$
blood	21 ± 3	31 ± 14
lung	23 ± 2	19 ± 6
liver	5.1 ± 0.9	6.9 ± 1.8
spleen	64 ± 5	20 ± 8
kidney	3.6 ± 0.6	0.05 ± 0.02
muscle	88 ± 28	74 ± 45
bone	41 ± 6	50 ± 13

[a]Data for ^{68}Ga-DOTA-$Z_{HER2:342}$ are taken from ref 22. Data are presented as average value for four mice with standard deviation.

In conclusion, the introduction of a triglutamyl linker between *N*-(4-fluorobenzylidine)oxime and the N-terminus of Affibody molecules provides a conjugate with a high (low picomolar) affinity. In mice, both hepatic and renal uptake of ^{18}F-FBO-E_3-PEP4313 was reduced ca. 2.7-fold in comparison with ^{18}F-FBO-PEP4313. Experiments in tumor-bearing mice confirmed that tumor uptake of ^{18}F-FBO-E_3-PEP4313 exceeds the uptake in both liver and kidneys already at 2 h after injection with good margin. This creates preconditions for improving contrast of imaging of abdominal metastases using Affibody molecules.

AUTHOR INFORMATION

Corresponding Author

*E-mail: vladimir.tolmachev@bms.uu.se.

Notes

The authors declare no competing financial interest.

ACKNOWLEDGMENTS

This research was financially supported by grants from Swedish Cancer Society (Cancerfonden), Swedish Research Council (Vetenskapsrådet) and the VINNOVA SAMBIO program.

REFERENCES

(1) Hanahan, D., and Weinberg, R. A. (2011) Hallmarks of cancer: the next generation. *Cell. 144*, 646−674.

(2) van Dongen, G. A., Poot, A. J., and Vugts, D. J. (2012) PET imaging with radiolabeled antibodies and tyrosine kinase inhibitors: immuno-PET and TKI-PET. *Tumour Biol. 33*, 607−615.

(3) Tolmachev, V., Stone-Elander, S., and Orlova, A. (2010) Current approaches to the use of radiolabeled tyrosine kinase-targeting drugs for patient stratification and treatment response monitoring: prospects and pitfalls. *Lancet Oncol. 11*, 992−1000.

(4) van Dongen, G. A., Visser, G. W., Lub-de Hooge, M. N., de Vries, E. G., and Perk, L. R. (2007) Immuno-PET: a navigator in monoclonal antibody development and applications. *Oncologist 12*, 1379−1389.

(5) McCabe, K. E., and Wu, A. M. (2010) Positive progress in immunoPET–not just a coincidence. *Cancer Biother. Radiopharm. 25*, 253−261.

(6) Schmidt, M. M., and Wittrup, K. D. (2009) A modeling analysis of the effects of molecular sizeand binding affinity on tumor targeting. *Mol. Cancer Ther. 8*, 2861−2871.

(7) Nygren, P. A. (2008) Alternative binding proteins: affibody binding proteins developed from a small three-helix bundle scaffold. *FEBS J. 275*, 2668−2676.

(8) Orlova, A., Magnusson, M., Eriksson, T. L., Nilsson, M., Larsson, B., Höidén-Guthenberg, I., Widström, C., Carlsson, J., Tolmachev, V.,

Ståhl, S., and Nilsson, F. Y. (2006) Tumor imaging using a picomolar affinity HER2 binding affibody molecule. *Cancer Res. 66*, 4339−4348.
(9) Tolmachev, V., Rosik, D., Wallberg, H., Sjoberg, A., Sandstrom, M., Hansson, M., Wennborg, A., and Orlova, A. (2010) Imaging of EGFR expression in murine xenografts using site-specifically labeled anti-EGFR 111In-DOTA-ZEGFR:2377 Affibody molecule: aspect of the injected tracer amount. *Eur. J. Nucl. Med. Mol. Imaging 37*, 613−622.
(10) Malm, M., Kronqvist, N., Lindberg, H., Gudmundsdotter, L., Bass, T., Frejd, F. Y., Höidén-Guthenberg, I., Varasteh, Z., Orlova, A., Tolmachev, V., Ståhl, S., and Löfblom, J. (2013) Inhibiting HER3-mediated tumor cell growth with affibody molecules engineered to low picomolar affinity by position-directed error-prone PCR-like diversification. *PLoS One 8*, e62791.
(11) Lindborg, M., Cortez, E., Hoiden-Guthenberg, I., Gunneriusson, E., von Hage, E., Syud, F., Morrison, M., Abrahmsen, L., Herne, N., Pietras, K., and Frejd, F. Y. (2011) Engineered high-affinity affibody molecules targeting platelet-derived growth factor receptor beta in vivo. *J. Mol. Biol. 407*, 298−315.
(12) Tolmachev, V., Malmberg, J., Hofstrom, C., Abrahmsen, L., Bergman, T., Sjoberg, A., Sandstrom, M., Graslund, T., and Orlova, A. (2012) Imaging of insulinlike growth factor type 1 receptor in prostate cancer xenografts using the affibody molecule 111In-DOTA-ZIGF1R:4551. *J. Nucl. Med. 53*, 90−97.
(13) Tolmachev, V. (2008) Imaging of HER-2 overexpression in tumors for guiding therapy. *Curr. Pharm. Des. 14*, 2999−3011.
(14) Baum, R. P., Prasad, V., Müller, D., Schuchardt, C., Orlova, A., Wennborg, A., Tolmachev, V., and Feldwisch, J. (2010) Molecular imaging of HER2-expressing malignant tumors in breast cancer patients using synthetic 111In- or 68Ga-labeled affibody molecules. *J. Nucl. Med. 51*, 892−897.
(15) Sandberg, D., Wennborg, A., Feldwisch, F., Tolmachev, V., Carlsson, J., Garske, U., Sörensen, J., and Lindman, H. (2012) First clinical observations of HER2 specific [111In]ABY-025 metastatic detection capability in females with metastatic breast cancer. *J. Nucl. Med. 53* (Supplement 1), 220.
(16) Tolmachev, V., and Orlova, A. (2010) Influence of labelling methods on biodistribution and imaging properties of radiolabelled peptides for visualisation of molecular therapeutic targets. *Curr. Med. Chem. 17*, 2636−5265.
(17) Wållberg, H., Grafström, J., Cheng, Q., Lu, L., Martinsson Ahlzén, H. S., Samén, E., Thorell, J. O., Johansson, K., Dunås, F., Olofsson, M. H., Stone-Elander, S., Arnér, E. S., and Ståhl, S. (2012) HER2-positive tumors imaged within 1 h using a site-specifically 11C-labeled Sel-tagged affibody molecule. *J. Nucl. Med. 53*, 1446−5143.
(18) Kramer-Marek, G., Kiesewetter, D. O., Martiniova, L., Jagoda, E., Lee, S. B., and Capala, J. (2008)) [(18F]FBEM-ZHER2:342-Affibody molecule-a new molecular tracer for in vivo monitoring of HER2 expression by positron emission tomography. *Eur. J. Nucl. Med. Mol. Imaging. 35*, 1008−1018.
(19) Namavari, M., Padilla De Jesus, O., Cheng, Z., De, A., Kovacs, E., Levi, J., Zhang, R., Hoerner, J. K., Grade, H., Syud, F. A., and Gambhir, S. S. (2008) Direct site-specific radiolabeling of an affibody protein with 4-[(18)F]fluorobenzaldehyde via oxime chemistry. *Mol. Imaging Biol. 10*, 177−181.
(20) Heskamp, S., Laverman, P., Rosik, D., Boschetti, F., van der Graaf, W. T., Oyen, W. J., van Laarhoven, H. W., Tolmachev, V., and Boerman, O. C. (2012) Imaging of human epidermal growth factor receptor type 2 expression with 18F-labeled affibody molecule ZHER2:2395 in a mouse model for ovarian cancer. *J. Nucl. Med. 53*, 146−153.
(21) Miao, Z., Ren, G., Liu, H., Jiang, L., and Cheng, Z. (2010) Small-animal PET imaging of human epidermal growth factor receptor positive tumor with a 64Cu labeled affibody protein. *Bioconjugate Chem. 21*, 947−954.
(22) Tolmachev, V., Velikyan, V., Sandström, M., and Orlova, A. (2010) A HER2-binding Affibody molecule labeled with 68Ga for PET imaging. Direct in vivo comparison with 111In-labelled analogue. *Eur. J. Nucl. Med. Mol. Imaging 37*, 1356−1367.
(23) Kramer-Marek, G., Shenoy, N., Seidel, J., Griffiths, G. L., Choyke, P., and Capala, J. (2011) 68Ga-DOTA-affibody molecule for in vivo assessment of HER2/neu expression with PET. *Eur. J. Nucl. Med. Mol. Imaging. 38*, 1967−1976.
(24) Mume, E., Orlova, A., Larsson, B., Nilsson, A. S., Nilsson, F. Y., Sjöberg, S., and Tolmachev, V. (2005) Evaluation of ((4-hydroxyphenyl)ethyl)maleimide for site-specific radiobromination of anti-HER2 affibody. *Bioconjugate Chem. 16*, 1547−1655.
(25) Orlova, A., Wållberg, H., Stone-Elander, S., and Tolmachev, V. (2009) On the selection of a tracer for PET imaging of HER2-expressing tumors: direct comparison of a 124I-labeled affibody molecule and trastuzumab in a murine xenograft model. *J. Nucl. Med. 50*, 417−425.
(26) Tolmachev, V., and Stone Elander, S. (2010) Radiolabelled proteins for Positron Emission Tomography: pros and cons of labeling methods. *Biochim. Biophys. Acta 1800*, 487−510.
(27) McBride, W. J., Sharkey, R. M., Karacay, H., D'Souza, C. A., Rossi, E. A., Laverman, P., Chang, C. H., Boerman, O .C., and Goldenberg, D. M. (2009) A novel method of 18F radiolabeling for PET. *J. Nucl. Med. 50*, 991−998.
(28) Glaser, M., and Arstad, E. (2007) "Click labeling" with 2-[18f]fluoroethylazide for positron emission tomography. *Bioconjugate Chem. 18*, 989−993.
(29) Campbell-Verduyn, L. S., Mirfeizi, L., Schoonen, A. K., Dierckx, R. A., Elsinga, P. H., and Feringa, B. L. (2011) Strain-promoted copper-free "click" chemistry for 18F radiolabeling of bombesin. *Angew. Chem., Int. Ed. 50*, 11117−11120.
(30) Li, Z., Cai, H., Hassink, M., Blackman, M. L., Brown, R. C., Conti, P. S., and Fox, J. M.. (2010) Tetrazine-trans-cyclooctene ligation for the rapid construction of 18F labeled probes. *Chem. Commun. 46*, 8043−8045.
(31) Poethko, T., Schottelius, M., Thumshirn, G., Hersel, U., Herz, M., Henriksen, G., Kessler, H., Schwaiger, M., and Wester, H. J. (2004) Two-step methodology for high-yield routine radiohalogenation of peptides: (18)F-labeled RGD and octreotide analogs. *J. Nucl. Med. 45*, 892−902.
(32) Cheng, Z., De Jesus, O. P., Namavari, M., De, A., Levi, J., Webster, J. M., Zhang, R., Lee, B., Syud, F. A., and Gambhir, S. S. (2008) Small-animal PET imaging of Human Epidermal Growth Factor Receptor Type 2 expression with site-specific 18F-labeled protein scaffold molecules. *J. Nucl. Med. 49*, 804−813.
(33) Miao, Z., Ren, G., Jiang, L., Liu, H., Webster, J. M., Zhang, R., Namavari, M., Gambhir, S.S ., Syud, F., and Cheng, Z. (2011) A novel 18F-labeled two-helix scaffold protein for PET imaging of HER2-positive tumor. *Eur. J. Nucl. Med. Mol. Imaging 38*, 1977−1984.
(34) Disibio, G., and French, S. W. (2008) Metastatic patterns of cancers: results from a large autopsy study. *Arch. Pathol. Lab. Med. 132*, 931−939.
(35) Rosik, D., Orlova, A., Malmberg, J., Altai, M., Varasteh, Z., Sandström, M., Eriksson Karlström, A., and Tolmachev, V. (2012) Direct comparison of 111In-labelled two-helix and three-helix Affibody molecules for in vivo molecular imaging. *Eur. J. Nucl. Med. Mol. Imaging 39*, 693−702.
(36) Hosseinimehr, S. J., Tolmachev, V., and Orlova, A. (2012) Factors influencing liver uptake of radiolabelled targeting protein and peptides: consideration for design of targeting conjugate peptide. *Drug Discovery Today 17*, 1224−1232.
(37) Tran, T., Engfeldt, T., Orlova, A., Sandström, M., Feldwisch, J., Abrahmsen, L., Wennborg, A., Tolmachev, V., and Eriksson Karlström, A. (2007) 99mTc-maEEE-ZHER2:342, an Affibody molecule-based tracer for detection of HER2-expression in malignant tumors. *Bioconjugate Chem. 18*, 1956−1964.
(38) Tolmachev, V., Hofström, C., Malmberg, J., Ahlgren, S., Hosseinimehr, S. J., Sandström, M., Abrahmsén, L., Orlova, A., and Gräslund, T. (2010) HEHEHE-Tagged affibody molecule may be purified by IMAC, is conveniently labeled with [99mTc(CO)3](+), and shows improved biodistribution with reduced hepatic radioactivity accumulation. *Bioconjugate Chem. 21*, 2013−2022.

(39) Tran, T. A., Rosik, D., Abrahmsén, L., Sandström, M., Sjöberg, A., Wållberg, H., Ahlgren, S., Orlova, A., and Tolmachev, V. (2009) Design, synthesis and biological evaluation of a HER2-specific affibody molecule for molecular imaging. *Eur. J. Nucl. Med. Mol. Imaging 36*, 1864−73.
(40) Engfeldt, T., Orlova, A., Tran, T., Bruskin, A., Widström, C., Eriksson Karlström, A., and Tolmachev, V. (2007) Imaging of HER2-expressing tumours using a synthetic Affibody molecule containing the 99mTc-chelating mercaptoacetyl-glycyl-glycyl-glycyl (MAG3) sequence. *Eur. J. Nucl. Med. Mol. Imaging 34*, 722−33.
(41) Tolmachev, V., Tran, T. A., Rosik, D., Abrahmsén, L., Sjöberg, A., and Orlova, A. (2012) Tumor targeting using Affibody molecules: interplay of affinity, target expression level and binding site composition. *J. Nucl. Med. 53*, 953−960.
(42) Wållberg, H., and Orlova, A. (2008) Slow internalization of anti-HER2 synthetic affibody monomer 111In-DOTA-ZHER2:342-pep2: implications for development of labeled tracers. *Cancer Biother. Radiopharm. 23*, 435−442.
(43) Strand, J., Honarvar, H., Perols, A., Orlova, A., Selvaraju, R. K., Karlström, A. E., and Tolmachev, V. (2013) Influence of macrocyclic chelators on the targeting properties of (68)Ga-labeled synthetic affibody molecules: comparison with (111)In-labeled counterparts. *PLoS One 8*, e70028.
(44) Behr, T. M., Goldenberg, D. M., and Becker, W. (1998) Reducing the renal uptake of radiolabeled antibody fragments and peptides for diagnosis and therapy: present status, future prospects and limitations. *Eur. J. Nucl. Med. 25*, 201−212.
(45) Pantelouris, E. M., and Lintern-Moore, S. (1978) Physiological Studies on the Nude Mouse. *The Nude Mouse in Experimental and Clinical Research* (Fogh, J., Ed.) pp 29−31, Chapter 3, Academic Press, New York.
(46) Engfeldt, T., Tran, T., Orlova, A., Widström, C., Feldwisch, J., Abrahmsen, L., Wennborg, A., Karlström, A. E., and Tolmachev, V. (2007) 99mTc-chelator engineering to improve tumour targeting properties of a HER2-specific Affibody molecule. *Eur. J. Nucl. Med. Mol. Imaging 34*, 1843−1453.
(47) Tran, T., Engfeldt, T., Orlova, A., Widström, C., Bruskin, A., Tolmachev, V., and Karlström, A. E. (2007) In vivo evaluation of cysteine-based chelators for attachment of 99mTc to tumor-targeting Affibody molecules. *Bioconjugate Chem. 18*, 549−658.
(48) Tran, T. A, Ekblad, T., Orlova, A., Sandström, M., Feldwisch, J., Wennborg, A., Abrahmsén, L., Tolmachev, V., and Eriksson Karlström, A. (2008) Effects of lysine-containing mercaptoacetyl-based chelators on the biodistribution of 99mTc-labeled anti-HER2 Affibody molecules. *Bioconjugate Chem. 19*, 2568−2576.